Discrete-time Control Contraction Metrics (DCCM) for Quasistatic Planar Pushing using Smoothed Dynamics

Shao Yuan Chew Chia *Harvard University*
Cambridge, MA
shaoyuan_chewchia@college.harvard.edu

Abstract—

I. INTRODUCTION

Planning and control through contact is an important capability in robotics. In order for robots to manipulate objects in their environment, they need to be able to reason about how to make and break contact. However, this has proved challenging for model-based methods due to two factors:

1) **Non-smooth or hybrid nature of contact dynamics**. Contact dynamics involve different modes of contact (e.g. sticking, sliding, no-contact), each with smooth but different dynamics and constraints. When switching between modes, the dynamics are discontinuous and change abruptly. This poses problems for gradient-based methods such as optimal control, as their locally linear models constructed using gradients quickly become inaccurate [1].

2) **Underactuatedness of the system**. Systems that involve contact are underactuated as the state of the unactuated objects cannot be controlled directly. Instead, control inputs to the robot are mediated through friction cones at contact points between the robot and the object, thus severely limiting the control authority of the inputs.

Current methods for model based planning and control through contact typically fall into one of three categories: methods that apply smoothing to the dynamics [1], [2], methods that explicitly enumerate the contact modes [3], and methods that implicitly reason about the contact modes [4]–[6]. Two methods that have been applied to the control of nonlinear underactuated systems are Linear Quadratic Regulator (LQR)-Trees and Control Contraction Metrics (CCMs). LQR-Trees use locally optimal linear control policies to stabilize planned trajectories. Each trajectory has a basin of attraction and these regions are pieced together to cover a larger region of state space. LQR Trees [7]. Control Contraction Metrics, first established in [8], were shown to be effective at controling underactuated systems in [9].

Control Contraction Metrics (CCM)s theoretically provide 4 key advantages over other control methods as described in [8]–[11]:

1) **Certificates of stability and convergence rates**. In general, nonlinear MPC does not provide guarantees on stability or performance. While Control Lyapunov Functions (CLFs) and LQR based methods can produce certificates, the guarantees provided by CCMs are not tied to specific equilbria or trajectories.

2) **Trajectory independent controllers**. CCMs generate controllers that stabilize every feasible trajectory in a region, while CLFs and LQR based methods require designing controllers for each trajectory and stitching them together to cover larger regions.

3) **Convex synthesis of the controller**. The control synthesis problem can be formulated as a convex optimization problem, which is easier to solve numerically and can leverage powerful tools like SOS programming.

4) **Faster online computation of the control law**. The online computation of the geodesic in CCMs is typically simpler than the nonlinear MPC optimal control problem.

In this paper we use the analytic smoothing of contact dynamics described in [1] to address the challenge of non-smoothness, and explore the effectiveness of building a Discrete-time Control Contraction Metric (DCCM) as demonstrated by [11] on top of that smoothed system to handle the underactuatedness and nonlinearity of the system. Our hope was that we would be able to synthesize a DCCM for a system with low amounts of smoothing and that this controller would also stabilize a "real-world" system with exact dynamics, however we did not manage to achieve that goal. We only managed to synthesize a controller that worked around a particular desired trajectory under significant smoothing, but are hopeful that our findings in this paper will serve as a good jumping off points for future work to realize the full potential of DCCMs applied to systems with contact.

II. PRELIMINARIES AND PROBLEM FORMULATION

A. Quasistatic Assumptions

We will assume that our system is quasistatic, meaning at each time step velocities and accelerations of the system are 0. This corresponds to having a high amount of damping and is a reasonable assumption in the 2D planar pushing setup where
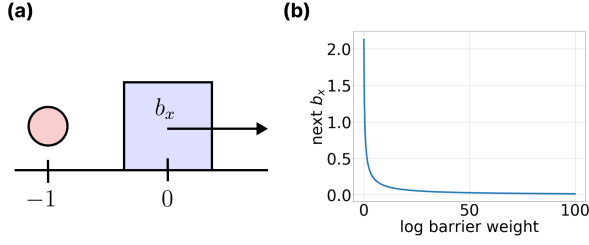
Fig. 1: Force at a distance effect of smoothed contact dynamics. (a) A system consisting of an actuated point finger at $x = -1$ and unactuated box at $x = 0$, (b) The next b_x after rolling out one step of the analytically smoothed dynamics with different log barrier weights.

we restrict pushing velocities to be low and there is a large amount of friction between the object and table surface. As a result, the state of our system only consists of positions.

B. Analytically Smoothed Contact Dynamics

In this work we use the analytically smoothed contact dynamics and corresponding simulator developed by [1]. Contact dynamics are formulated as an unconstrained convex program where the contact and friction contraints are moved into the objective function using a log barrier function. The effect of this is that there is a log barrier penalty for violating the contact constraints. Constraints can exert force even if they are not active and this translates to producing a force at a distance.

We plot the force at a distance effect of the smoothed contact dynamics in Figure 1. We see that for a high weight, which corresponds to a small force at a distance, the next b_x is close to 0, but as the log barrier weight decreases, the box is pushed further to the right.

C. Planar Pushing System

The state of

$$x = \begin{bmatrix} b_x & b_y & b_\theta & s_x & s_y \end{bmatrix}^\top \qquad (1)$$

control input u are absolute position commands for the sphere

$$u = \begin{bmatrix} u_x \\ u_y \end{bmatrix} \qquad (2)$$

The system evolves in nonlinearly in discrete time and is control affine. The dynamics are defined as

$$x_{k+1} = f(x_k) + g(x_k)u_k \qquad (3)$$

where f and g are smooth functions due to the smoothing of the contact dynamics described in the previous section.

The differential dynamics are defined as

$$\delta_{x_k} = A(x_k)\delta_{x_k} + B(x_k)\delta_{u_k} \qquad (4)$$

where $A(x_k) = \frac{\partial(f(x_k)+g(x_k)u_k)}{\partial x_k} \in \mathbb{R}^{5\times5}$ and $B(x_k) = \frac{\partial(f(x_k)+g(x_k)u_k)}{\partial u_k} \in \mathbb{R}^{5\times2}$ are the Jacobians of the dynamics.

We can define the state feedback control law

$$\delta_{u_k} = K(x_k)\delta_{x_k} \qquad (5)$$

where K is the state dependent feedback gain matrix.

Generalized infinitesimal squared distance in the positive definite metric M is denoted V_k

$$V_k = \delta_{x_k}^\top M_k \delta_{x_k} \qquad (6)$$

And by substituting the differential dynamics and control law, we can see that the generalized infinitesimal squared distance at the next time step is

$$\begin{aligned} V_{k+1} &= \delta_{x_{k+1}}^\top M_{k+1} \delta_{x_{k+1}} \\ &= \delta_{x_k}^\top (A_k + B_k K_k)^\top M_{k+1}(A_k + B_k K_k)\delta_{x_k} \end{aligned} \qquad (7)$$

The contraction condition can then be expressed as

$$V_{k+1} - V_k \leq -\beta V_k < 0 \qquad (8)$$

which simplifies to

$$(A_k + B_k K_k)^\top M_{k+1}(A_k + B_k K_k) - (1 - \beta)M_k < 0 \quad (9)$$

[11] showed that equation 9 can be transformed via Schur's complement (among other transformations) into

$$\begin{bmatrix} W_{k+1} & A_k + B_k L_k \\ (A_k + B_k L_k)^\top & (1 - \beta)W_k \end{bmatrix} > 0 \qquad (10)$$

where $W := M^{-1}$ and $L := KW$

III. METHODS

A. Contraction Metric and Controller Synthesis

1) Sum of Squares (SOS) Programming: In order to synthesize the contraction metric and controller, we use the SOS programming framework described in [11] with some slight modifications.

$$\begin{aligned} &\min_{l_c, w_c, r} r \\ &s.t. \forall k, w^\top \Omega w - r w^\top w \in \Sigma(x_k, u_k, w) \\ &r \geq 0.1 \end{aligned} \qquad (11)$$

where $\Sigma(x_k, u_k, w)$ is the set of SOS polynomials that satisfy the contraction condition in equation 10. l_c are the polynomial coefficients of L and w_c are the polynomial coefficients of W.

$$\Omega = \begin{bmatrix} W_{k+1} & A_k + B_k L_k \\ (A_k + B_k L_k)^\top & (1 - \beta)W_k \end{bmatrix}$$

$$W_k = \begin{bmatrix} W_{11_k} & W_{12_k} & W_{13_k} & W_{14_k} & W_{15_k} \\ W_{12_k} & W_{22_k} & W_{23_k} & W_{24_k} & W_{25_k} \\ W_{13_k} & W_{23_k} & W_{33_k} & W_{34_k} & W_{35_k} \\ W_{14_k} & W_{24_k} & W_{34_k} & W_{44_k} & W_{45_k} \\ W_{15_k} & W_{25_k} & W_{35_k} & W_{45_k} & W_{55_k} \end{bmatrix} \qquad (12)$$

$$L_k = \begin{bmatrix} L_{11_k} & L_{12_k} & L_{13_k} & L_{14_k} & L_{15_k} \\ L_{21_k} & L_{22_k} & L_{23_k} & L_{24_k} & L_{25_k} \end{bmatrix}$$

each $W_{..k} = w_{..c}v(x_k)$ is a polynomial constructed from the row vector of coefficients of $w_{..c}$ and the monomial basis vector $v(x_k)$. For example, if the degree of the polynomial is chosen to be 4,

$$v(x_k) = [x_{k_4}^4, x_{k_3}x_{k_4}^3, x_{k_3}^2x_{k_4}^2, \cdots, x_{k_1}, x_{k_0}, 1] \qquad (13)$$

where $v(x_k)$ has 126 elements. $L_{..k} = l_{..c}v(x_k)$ is similarly defined.

In general, the dimensions of the matrices are as follows: $\Omega : 2 \cdot dim(x) \times 2 \cdot dim(x), W : dim(x) \times dim(x), L : dim(u) \times dim(x)$

We note the difference in the way we use the slack variable r compared to [11]. In [11], the constraints on the optimization program are $w^\top \Omega w - rI \in \Sigma(x_k, u_k, w), r \geq 0$. In practice we found that in some cases, especially when generating a higher degree metric, that the solver would return a trivial solution where r, w_c and l_c are extremely small numbers (on the order of $1e-17$). By setting a higher bound on r, we force the solver to find a solution where the contraction condition is satisfied with a greater buffer and the returned coefficients of w_c and l_c are larger.

Another difference is that we do not have closed form equations for the A and B matrices which would allow us to enforce the contraction conditions over all states. Instead, we sample a set of state, control action pairs and enforce the contraction condition over these samples. We use the contact dynamics solver described in [1] to calculate the next state x_{k+1}, and the Jacobians A_k and B_k, for each sample of the current state x_k and control action u_k, and substitute these values into the constraints in optimization program (11). Since M is smooth, we can expect the contraction condition to be satisfied over at least a small local region around each sample. However, if the samples are too sparse, the contraction condition may not be satisfied over all the states around the desired trajectory.

We solve this SOS program using Drake's Mathematical Program [12], which uses Mosek under the hood to solve this Semidefinite Program (SDP).

2) Sampling Strategy: To get a contraction metric valid over the entire state space we would have to densely sample the entire state space. However, the available RAM on the machine sets an upper bound of the size of the optmization program, which for a monomial basis of degree 4, was around 2000 samples. Thus, to get a contraction metric and controller that had good performance at least in the vicinity of the desired trajectory, we only sampled states and control actions from a small region around the desired trajectory. This is a clear limitation of the current approach and future work would involve finding a way to enforce the contraction condition over a larger portion of state space.

B. Online Geodesic and Controller Computation

With the contraction metric synthesized, we now need to compute the control action that enforces the contraction condition.

For a smooth curve $c(s), s \in [0, 1]$ that connects two points in state space x_0 and x_1, [8] defines the Riemannian length and energy of the curve as

$$L(c) = \int_0^1 \sqrt{\frac{\partial c(s)}{\partial s}^\top M(c(s)) \frac{\partial c(s)}{\partial s}} ds \tag{14}$$

$$E(c) = \int_0^1 L(c)^2 ds$$

The geodesic $\gamma(x_0, x_1)$ is the curve that minimizes the Riemanian length and energy between x_0 and x_1

$$\gamma(x_0, x_1) = \underset{c}{\mathrm{argmin}}\, L(c)$$
$$= \arg\min_c E(c) \tag{15}$$

By the contraction condition we enforced, we see that the Riemanian energy of geodesic decreases exponentially as the system evolves and thus can be thought of as an incremental Lyapunov function [8]. In order to numerically approximate the geodesic $\gamma(x_k^*, x_k)$, we discretize the curve into N segments and solve the following optimization program

$$\bar{\gamma}(x_k^*, x_k) = \underset{\substack{x[\cdot], \Delta x_s[\cdot], \\ \Delta s[\cdot], m[\cdot], y[\cdot]}}{\mathrm{argmin}} \sum_{i=0}^{N-1} y[i] + \Delta s[i]^2$$

$$s.t. \forall i, y \geq \Delta s[i] \Delta x_s[i]^\top M(m[i]) \Delta x_s[i]$$
$$x[0] = x_k^*, \quad x[N] = x_k$$
$$\forall i, x[i+1] = x[i] + \Delta x_s[i] \Delta s[i]$$
$$\forall i, \Delta s[i] > 0, \quad \sum_{i=0}^{N-1} \Delta s[i] = 1$$
$$\forall i, M(m[i]) W(x[i]) = I$$

$$\tag{16}$$

where $x[i]$ is the state at the start of the ith segment of the geodesic, $\Delta s[i]$ is a small positive scalar, $\Delta x_s[i]$ is the discretized displacement vector, $y[i]$ is a slack variable that represents the Riemanian energy and N is the number of segments the γ is discretized into. $m[i]$ is a slack variable introduced such that the 5×5 symbolic matrix $W(x[i])$ does not need to be explicitly inverted which was found to be a severe computational bottleneck. The constraint $M(m[i])W(x[i]) = I$ is a surrogate for enforcing $M(m[i]) = W(x[i])^{-1}$. Adding $\Delta s[i]^2$ to the objective serves to spread out the discretized points evenly along the geodesic.

As this is a non-convex program, we use Drake, this time using SNOPT under the hood [12].

With the geodesic $\bar{\gamma}(x_k^*, x_k)$ computed, we can compute the control action u_k that enforces the contraction condition

$$u_k = u_k^* + \sum_{i=0}^{N-1} \Delta s[i] K(x[i]) \Delta x_s[i]$$
$$= u_k^* + \sum_{i=0}^{N-1} \Delta s[i] L(x[i]) W(x[i])^{-1} \Delta x_s[i] \tag{17}$$

An important point to note is that the integration is done from x_k^* to x_k and not the other way around. While it might seem intuitive that we want to calculate the δ_u that brings the system from x_k to x_k^*, this is actually not the right way to think about it. First, the δ_u in equation 5 does not lead to a change in state δ_x on the right side of the same equation. Instead, 5 tells us for a change in state δ_x from a nominal trajectory, what is the corresponding δ_u that enforces the contraction condition. In this case, the nominal trajectory is x^* and u^*, thus to calculate the δ_u that enforces the contraction condition, we need to integrate from x_k^* to x_k.

IV. Experimental Setup

A. Creating Feasible Desired Trajectories

To create the desired trajectory, we first parameterised an arbitrary circular trajectory with the robot "behind" the object at each time step and the object slowly rotating as it travelled around the circle. We then rolled out the dynamics from the initial condition, using the position of the robot at the next time step as the open loop position command for the robot and recorded the actual positions of the object under this open loop control. We created two feasible circular trajectories of slightly different radius in this way and spliced them together in the middle in order to introduce a step change in the desired trajectory. Finally, we introduce an additional initial disturbance by adding an offset to the initial state from the first state of the desired trajectory. We do this process twice to create desired trajectories for both the log barrier weight 10 and 100 levels of smoothing.

V. Results and Discussion

Our original goal was to synthesize a DCCM with a small amount of smoothing that would transfer well to stabilizing the real system to arbitrary feasible desired trajectories under non-smooth, exact contact dynamics. Unfortunately, we were not able to achieve this goal. We find that when using a small amount of smoothing, a higher degree monomial basis was required to enforce the contraction condition across all samples. Furthermore, since the dynamics were less smooth, a greater density of samples was required in order for the contraction condition to hold around the desired trajectory. This can be seen from the result in table (I) where even though we were able to synthesize DCCMs for 500 samples for both log barrier weights, the DCCM for log barrier weight 10 worked while the DCCM for log barrier weight 100 did not.

Both of these factors (requiring a higher degree, and more samples) led to the optimization (11) being intractable due to the computer used running out of RAM. Ultimately we were only able to find a stabilizing controller for a log barrier weight of 10, which corresponds to the robot exerting 0.1 Newtons of force on an object that is 1 meter away.

A. Effect of different parameters

B. Degree of metric on

Higher degree means its more able to find a contraction metric for a system with more "warped" dynamics, i.e. if there is less smoothing.

But higher degree also means less samples can be used, and increased computation time.

C. Effect of number of samples on controller performance

VI. Conclusion and Future Work

More work needs to be done to realize the full benefits of applying the Control Contraction Metric Framework to the problem of control through contact.

Log Barrier Weight	Deg.	# Samples	100	500	1000	2000	3000
10	4	Synthesizes	✓	✓	✓	✓	!
		Stabilzes	✗	✓	✓	✓	-
	6	Synthesizes	✓	✓	!	-	-
		Stabilizes	✗	✗	-	-	-
100	4	Synthesizes	✓	✓	✗	-	-
		Stabilzes	✗	✗	-	-	-
	6	Synthesizes	✓	✓	!	-	-
		Stabilizes	✗	✗	-	-	-

TABLE I: Feasibility (whether a DCCM can be synthesized) and performance (whether the found DCCM stabilizes to the desired trajectory) across different log barrier weights (10 is high smoothing, 100 is low smoothing), degree of monomial basis used, and number of sampled points at which the contraction condition is enforced. Symbols: ✓(succeeds), ✗(fails), ! (program crashes), - (did not/could not run test).

Same controller across different trajectories - this was not realized in our implementation because of the sampling technique used.

Convex synthesis - high degree SOS polynomial required

Certificates of stability and convergence rates - need arguments about samping density, and also bounding the difference between smoothed and exact dynamics.

faster online computation - explore other methods for solving the geodesic that don't involve inverting the symbolic matrix.

References

[1] T. Pang, H. J. T. Suh, L. Yang, and R. Tedrake. (Feb. 27, 2023). Global Planning for Contact-Rich Manipulation via Local Smoothing of Quasi-dynamic Contact Models. Comment: The first two authors contributed equally to this work. arXiv: 2206.10787 [cs], [Online]. Available: http://arxiv.org/abs/2206.10787 (visited on 03/15/2023), preprint.

[2] D. E. Stewart and M. Anitescu, "Optimal control of systems with discontinuous differential equations," *Numerische Mathematik*, vol. 114, no. 4, pp. 653–695, Feb. 1, 2010, ISSN: 0945-3245. DOI: 10.1007/s00211-009-0262-2. [Online]. Available: https://doi.org/10.1007/s00211-009-0262-2 (visited on 05/12/2023).

[3] F. R. Hogan and A. Rodriguez. (Nov. 24, 2016). Feedback Control of the Pusher-Slider System: A Story of Hybrid and Underactuated Contact Dynamics. arXiv: 1611.08268 [cs], [Online]. Available: http://arxiv.org/abs/1611.08268 (visited on 05/12/2023), preprint.

[4] J.-P. Sleiman, J. Carius, R. Grandia, M. Wermelinger, and M. Hutter, "Contact-Implicit Trajectory Optimization for Dynamic Object Manipulation," in *2019 IEEE/RSJ International Conference on Intelligent Robots and Systems (IROS)*, Comment: 8 Pages, 10 Figures. Submitted to the International Conference on

Intelligent Robots and Systems (IROS), 2019, Nov. 2019, pp. 6814–6821. DOI: 10.1109/IROS40897.2019.8968194. arXiv: 2103.01104 `[cs]`. [Online]. Available: http://arxiv.org/abs/2103.01104 (visited on 03/17/2023).

[5] K. Nakatsuru, W. Wan, and K. Harada. (Feb. 25, 2023). Implicit Contact-Rich Manipulation Planning for a Manipulator with Insufficient Payload. arXiv: 2302.13212 `[cs]`, [Online]. Available: http://arxiv.org/abs/2302.13212 (visited on 03/17/2023), preprint.

[6] M. Posa, C. Cantu, and R. Tedrake, "A direct method for trajectory optimization of rigid bodies through contact," *International Journal of Robotics Research*, vol. 33, no. 1, pp. 69–81, Jan. 1, 2014, ISSN: 0278-3649. DOI: 10.1177/0278364913506757. [Online]. Available: https://doi.org/10.1177/0278364913506757 (visited on 03/17/2023).

[7] R. Tedrake, I. R. Manchester, M. Tobenkin, and J. W. Roberts, "LQR-trees: Feedback Motion Planning via Sums-of-Squares Verification," *The International Journal of Robotics Research*, vol. 29, no. 8, pp. 1038–1052, Jul. 1, 2010, ISSN: 0278-3649. DOI: 10.1177/0278364910369189. [Online]. Available: https://doi.org/10.1177/0278364910369189 (visited on 05/13/2023).

[8] I. R. Manchester and J.-J. E. Slotine, "Control Contraction Metrics: Convex and Intrinsic Criteria for Nonlinear Feedback Design," *IEEE Transactions on Automatic Control*, vol. 62, no. 6, pp. 3046–3053, Jun. 2017, ISSN: 1558-2523. DOI: 10.1109/TAC.2017.2668380.

[9] I. R. Manchester, J. Z. Tang, and J.-J. E. Slotine, "Unifying Robot Trajectory Tracking with Control Contraction Metrics," in *Robotics Research: Volume 2*, ser. Springer Proceedings in Advanced Robotics, A. Bicchi and W. Burgard, Eds., Cham: Springer International Publishing, 2018, pp. 403–418, ISBN: 978-3-319-60916-4. DOI: 10.1007/978-3-319-60916-4_23. [Online]. Available: https://doi.org/10.1007/978-3-319-60916-4_23 (visited on 05/05/2023).

[10] S. Singh, A. Majumdar, J.-J. Slotine, and M. Pavone, "Robust Online Motion Planning via Contraction Theory and Convex Optimization," May 29, 2017. DOI: 10.1109/ICRA.2017.7989693.

[11] L. Wei, R. Mccloy, and J. Bao, "Control Contraction Metric Synthesis for Discrete-time Nonlinear Systems," *IFAC-PapersOnLine*, 16th IFAC Symposium on Advanced Control of Chemical Processes ADCHEM 2021, vol. 54, no. 3, pp. 661–666, Jan. 1, 2021, ISSN: 2405-8963. DOI: 10.1016/j.ifacol.2021.08.317. [Online]. Available: https://www.sciencedirect.com/science/article/pii/S2405896321010910 (visited on 04/16/2023).

[12] R. T. a. the Drake Development Team. (2019). Drake: Model-Based Design and Verification for Robotics, [Online]. Available: https://drake.mit.edu/ (visited on 05/10/2023).